EFFECT OF NOZZLE LENGTH ON GAS ENTRAINMENT CHARACTERISTICS OF VERTICAL LIQUID JET

AKIRA OHKAWA, DAISUKE KUSABIRAKI AND NOBUYUKI SAKAI
Department of Chemical Engineering, Niigata University, Niigata 950-21

Key Words: Vertical Liquid Jet, Nozzle Length, Bubble Penetration Depth, Gas Entrainment Rate, Jet Surface Change

For a vertical plunging liquid jet system using nozzles which had various values of the length-to-diameter ratio L_n/D_n, characteristics such as the bubble penetration depth Z and the gas entrainment rate Q_g were studied experimentally in an air-water system. When nozzles of an L_n/D_n ratio exceeding 15 were employed, the values of Z and Q_g were confirmed to be almost independent of L_n/D_n. Empirical correlations for predicting Z and Q_g are also presented.

Introduction

An aeration system based on gas entrainment by a liquid jet is attractive compared to conventional gas-sparging systems because of its simplicity in construction and operation.[2] The earlier researchers adopted four operating variables which affect the gas entrainment characteristics of a liquid jet. They are: nozzle diameter, nozzle velocity, nozzle height, and nozzle angle. However, it is insufficient to investigate or discuss the characteristics of the liquid jet by these four factors only. An important factor that cannot be overlooked is differences in the nozzle design, especially the nozzle length-to-diameter ratio L_n/D_n.[4,5,13,21] Reviewing the existing studies on inclined or vertical plunging water jets, most of these works were carried out in long nozzles which had a value of L_n/D_n exceeding 50.[8,9,11,17-21] In such systems, useful information is available on the gas entrainment characteristics. In contrast, there are few studies in which the characteristics of the liquid jet were investigated over a wide range of L_n/D_n. Considering practical application of the jet aeration system, it is assumed that there are cases where a long nozzle with a large L_n/D_n ratio cannot be used due to the structural limitation of the reactors or difficulties in the piping and the liquid feeding, etc. For example, consider the case of using a nozzle of 0.02 m diameter: the nozzle must be longer than 1.0 m to satisfy the condition of L_n/D_n greater than 50. Long nozzles of a large L_n/D_n seems to be of no practical use. That suggests the necessity of a study to clarify the range of effective L_n/D_n ratio of the nozzle to be used. The bubble penetration depth Z and the gas entrainment rate Q_g in the vertical jet system using short nozzles of $L_n/D_n=5$ were reported in the previous work.[15] In the present study, the relationship between Z or Q_g and the operating conditions in vertical jet systems was investigated experimentally by varying widely the L_n/D_n ratio. Also, to obtain a clearer view of the suggestions made by some authors that when the liquid jet is discharged from the nozzle into a gas phase a change of the jet occurs[13] and that the jet surface change affects the gas entrainment,[4,7,12,14] the change of the jet with variation of operating conditions was observed, and some studies were made of the relation between these changes and the gas entrainment behavior.

Received October 29, 1986. Correspondence concerning this article should be addressed to A. Ohkawa.

1. Experimental

The experimental apparatus was almost the same as that employed in the previous work.[15] The apparatus consisted of a liquid pump, a straight cylindrical nozzle (PVC) with inside diameter D_n between 0.007 and 0.017 m, and a bath of height 1.0 m and section 1.0 m by 0.65 m. The jet velocity V_n was varied from 2.0 to 13.5 m/s, depending on D_n. The range of L_n/D_n ratio variation was between 5 and 70. The nozzle height H_n from the bath surface to the nozzle exit ranged from 0.025 to 0.75 m. The value of Z was measured by a scale fitted to the bath wall. In measuring the gas entrainment rate Q_g, the same volume of liquid as that of the entrained gas into the length-variable cylinder having a cap was introduced into a replacement vessel. By measuring the volume of liquid replaced by the entrained gas, the volumetric rate Q_g of entrained gas was determined. Additional details of the apparatus and procedures were shown in the previous paper.[15] The change of the jet surface was observed by taking photographs. All the

experiments were carried out at 293 K with an air–water system.

2. Results and Discussion

2.1 Bubble penetration depth Z

In our previous work,[15] the choice of non-dimensional parameters to be employed in plotting the data of Z was made by referring to a theoretical analysis of the momentum equation for the axisymmetric submerged jet[1] analogous to the vertical plunging jet system. And the relationship between Z and the operating conditions when nozzles having a constant L_n/D_n were employed was derived as an expression of functional form:

$$Z/D_n = \text{func.}(F_r, H_n/D_n) \tag{1}$$

The effect of L_n/D_n ratio on the change of the dimensionless bubble penetration depth Z/D_n was further investigated, along with the effects of the Froude number F_r $(=V_n/\sqrt{gD_n})$ and the ratio of nozzle height to diameter, H_n/D_n. **Figure 1** shows the typical relationship between Z/D_n and L_n/D_n. As can be seen from these results, Z/D_n decreases with L_n/D_n, if the L_n/D_n ratio is smaller than 15, but is almost constant above this range. **Figure 2** shows the effect of H_n/D_n on Z/D_n. The effect of H_n/D_n was the same as that observed for the nozzles of $L_n/D_n=5$.[15] That is, regardless of L_n/D_n, Z/D_n at H_n/D_n below 20 tended to decrease with H_n/D_n and be almost constant above that range. Moreover, in experiments using short nozzles of D_n from 0.001 to 0.004 m but of unknown values of L_n/D_n, Suciu and Smigelschi[16] observed that Z/D_n at H_n/D_n above 20 becomes almost independent of H_n/D_n, similarly to our results.

2.2 Correlation of Z

The bubble penetration depth Z when the short nozzles of $L_n/D_n=5$ were employed was shown to be represented by the following form.[15]

$$Z/D_n=(H_n/D_n)^A 10^{f(F_r)} \tag{2}$$

where A is constant and $f(F_r)$ is a function of F_r. A correlation of Z/D_n in which the effect of L_n/D_n was further taken into consideration on the right-hand side of Eq. (2) was carried out, by utilizing such results as shown in Figs. 1 and 2. As plotted in **Fig. 3**, the values of Z/D_n were correlated by the following form within 15% error.

$$Z/D_n=(L_n/D_n)^\alpha(H_n/D_n)^\beta 10^{f(F_r)} \tag{3}$$

$$f(F_r)=\gamma+\delta(\text{Log}\,F_r)+\xi(\text{Log}\,F_r)^2 \tag{4}$$

The values of empirical constants α, β, γ, δ and ξ, which change depending on the range of L_n/D_n and H_n/D_n, are summarized in **Table 1**. Equations (3) and (4) are applicable when L_n/D_n is 5–70, H_n/D_n is 1.4–108, and F_r is 4.8–51.5.

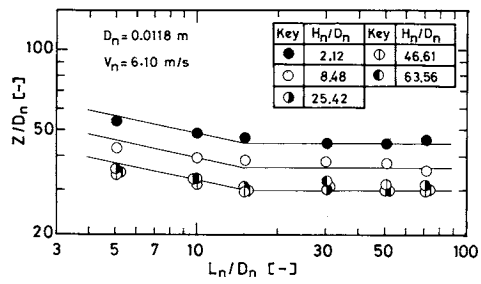

Fig. 1. Effect of L_n/D_n on Z/D_n.

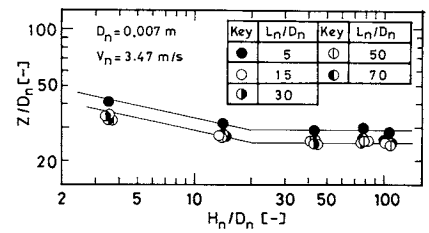

Fig. 2. Effect of H_n/D_n on Z/D_n.

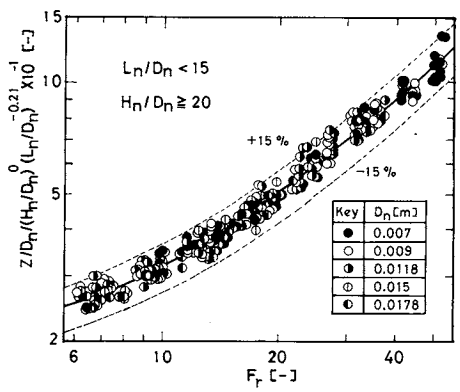

Fig. 3. Empirical correlation of Z/D_n.

Table 1. Values of α, β, γ, δ and ξ in Eqs. (3) and (4)

L_n/D_n [—]	H_n/D_n [—]	α [—]	β [—]	γ [—]	δ [—]	ξ [—]
5–15	1.4– 20	−0.21	−0.21	1.55	−0.15	0.37
	20 –107	−0.21	0	1.27	−0.09	0.32
15–70	1.4– 20	0	−0.21	1.26	−0.06	0.34
	20 –107	0	0	1.09	−0.14	0.35

Some reports have dealt with Z in vertical jet systems.[6,16,20] However, values of Z obtained in the system using nozzles for which the L_n/D_n ratio was specified have been reported only by Van de Sande and Smith.[20] They employed vertical nozzles of D_n from 0.0039 to 0.012 m which had a value of L_n/D_n exceeding 50 and measured Z at $H_n=0.2$ m and at V_n below 14 m/s. **Figure 4** shows a comparison of the results calculated with those observed.[20] Good coincidence can be seen.

2.3 Gas entrainment rate Q_g

In the previous paper,[15] the dimensionless gas

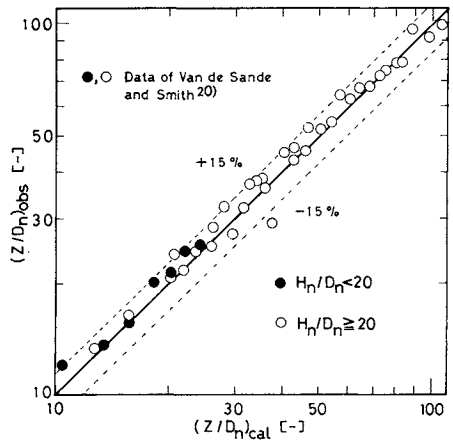

Fig. 4. Comparison of Z/D_n calculated from Eqs. (3) and (4) with values obtained by Van de Sande and Smith.[20]

entrainment rate Q_g/Q_L in nozzles having a constant L_n/D_n was shown as a function of F_r, H_n/D_n and the Ohnesorge number O_h $(=\mu\sqrt{\rho\sigma D_n})$.

$$Q_g/Q_L = \text{func.}(F_r, O_h, H_n/D_n) \tag{5}$$

The effect of L_n/D_n on Q_g/Q_L was further investigated. **Figure 5** shows the typical relationship between Q_g/Q_L and F_r. Q_g/Q_L is found to increase with F_r and H_n/D_n, but their rate of increase differs in the ranges of F_r below and above 20 at which V_n is about 5 m/s. For the effect of L_n/D_n and H_n/D_n, on the other hand, Q_g/Q_L when the nozzle of a large L_n/D_n is employed at a large H_n/D_n tended to increase linearly with F_r (Figs. 5b and 5c). **Figure 6** shows the typical relationship between Q_g/Q_L and L_n/D_n. These results indicate that Q_g/Q_L increases with increase of L_n/D_n, if the L_n/D_n ratio is smaller than 15, but is almost constant above this range.

2.4 Correlation of Q_g

From Fig. 5, the following functional form can be derived.

$$Q_g/Q_L \propto F_r^{f(H_n/D_n)} \tag{6}$$

Also, from the results for the range of L_n/D_n below 15 in Fig. 6, the relationships of Eqs. (7) and (8) which depend on the range of V_n are obtained.

$$Q_g/Q_L \propto (L_n/D_n)^{0.49} (V_n < 5\,\text{m/s}) \tag{7}$$

$$Q_g Q_L \propto (L_n/D_n)^{0.31} (V_n \geqq 5\,\text{m/s}) \tag{8}$$

Considering further the effects of H_n/D_n and O_h, the final correlation was carried out. As seen in an example of **Fig. 7**, Q_g/Q_L could be correlated by the following form within 30% error.

$$Q_g/Q_L = aF_r^{f(H_n/D_n)} O_h^b (H_n/D_n)^c (L_n/D_n)^d \tag{9}$$

$$f(H_n/D_n) = e(H_n/D_n)^f \tag{10}$$

The values of empirical constants a, b, c, d, e and f in Eqs. (9) and (10) which change depending on the

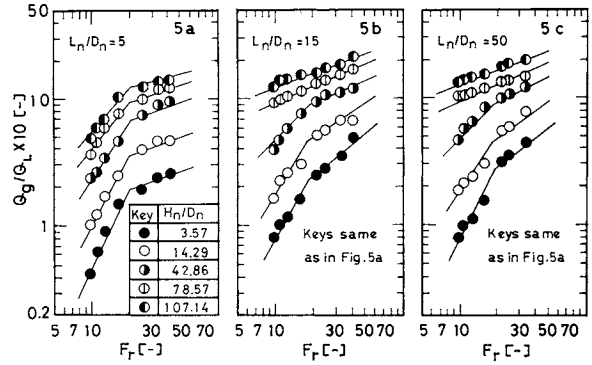

Fig. 5. Relationship between Q_g/Q_L and F_r for nozzles of $D_n = 0.007$ m.

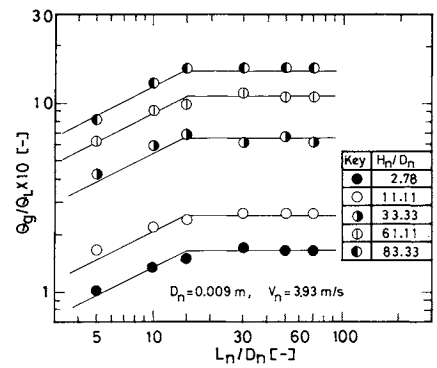

Fig. 6. Effect of L_n/D_n on Q_g/Q_L.

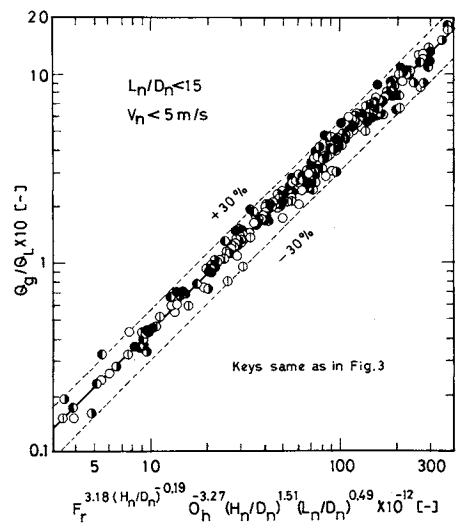

Fig. 7. Empirical correlation of Q_g/Q_L.

range of L_n/D_n and V_n are summarized in **Table 2**. Equations (2) and (10) are applicable when F_r is 4.8–51.5; H_n/D_n is 1.4–108; O_h is 8.82×10^{-4}–1.41×10^{-3}; and L_n/D_n is 5–70.

Recently, Van de Sande[19] proposed Eq. (11) for predicting Q_g/Q_L in the vertical water jet system, by utilizing the data of inclined jets using nozzles of $L_n/D_n \geqq 50$.

$$Q_g/Q_L = 0.04F_r^{0.56}(H_n/D_n)^{0.4} \tag{11}$$

Table 2. Values of a, b, c, d, e and f in Eqs. (9) and (10)

L_n/D_n [—]	V_n [m/s]	a [—]	b [—]	c [—]	d [—]	e [—]	f [—]
5–15	2–5	4.33×10^{-15}	−3.27	1.51	0.49	3.18	−0.19
	5–13.5	2.57×10^{-4}	−0.55	0.84	0.31	5.98×10^{-1}	−0.25
15–70	2–5	1.09×10^{-9}	−1.96	1.51	0	2.22	−0.34
	5–13.5	1.47×10^{-3}	−0.30	0.84	0	9.37×10^{-1}	−0.21

Bin[3] also has discussed the applicability of Eq. (11) to the results obtained from other available data on inclined jets. **Figure 8** shows a comparison between Q_g/Q_L values calculated from Eq. (11) and those observed in the present work and in a CO_2–water system ($D_n=0.0028$–0.0073 m, $H_n=0.02$–0.25 m and $V_n=2.0$–12.4).[22] As can be seen from Fig. 8, it is clear that Eq. (11) cannot be applied to all regions of gas entrainment. This is considered to be mainly due to the situation that Eq. (11) was based not on data actually measured but on data obtained by extrapolating those of inclined jets to the angle of 90°. **Figure 9** then shows a comparison of the observed Q_g/Q_L values[22] with those calculated from the present correlations. The data ($D_n=0.0057$ m, $H_n=0.1$ m and $V_n=5$–10 m/s)[22] in an aqueous CH_3COOH solution (0.1–10.0 vol%) system are also plotted. According to these results, Eqs. (9) and (10) seem to be valid for predicting not only the entrainment rate of CO_2 in water but also that in an aqueous CH_3COOH solution when vertical nozzles with various L_n/D_n ratios are employed.

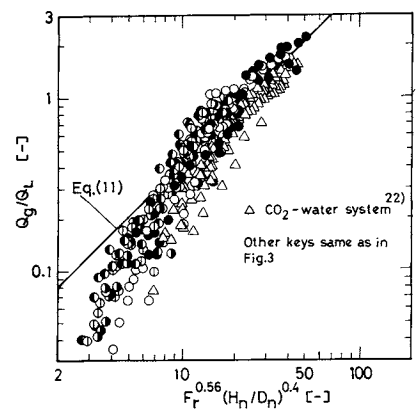

Fig. 8. Comparison of Q_g/Q_L calculated from Eq. (11) with values obtained in this work and in a CO_2–water system.[22]

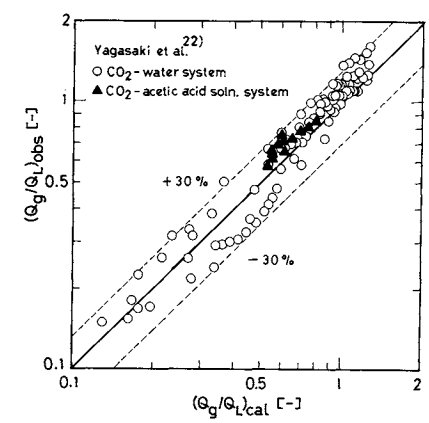

Fig. 9. Comparison of Q_g/Q_L calculated from Eqs. (9) and (10) with values obtained by Yagasaki and Kuzuoka.[22]

2.5 Change of jet surface

Figure 10 shows typical photographs of the jet. The jet type observed within the present experimental conditions was similar to the types (A), (B), (C) and (D) shown in Fig. 10. Moreover, no break-up of liquid jets occurred. **Figure 11** shows some typical patterns of jet surface obtained by photographic observations. For the change of jet surface with H_n/D_n, the jet of types (A) and (B) was found to be produced at H_n/D_n below 20 and that of types (C) and (D) above 20. This value of 20 corresponds to the transition H_n/D_n value on the change of Z/D_n as shown in Fig. 2. For the effect of V_n, as seen in the change of (A)→(B) or (C)→(D), the surface disturbance or the sinuosity, etc. became large gradually with increasing V_n. But, their way of changing differed slightly depending on the range of V_n. That is, the degree of their surface changes at V_n above about 5 m/s tended to be on the whole smaller than that below 5 m/s. In Fig. 5a, the increasing tendency of Q_g/Q_L at V_n exceeding 5 m/s was shown to be small compared to that below this range. One of the reasons for this seems to be related to the differences in jet surface change as observed above. On the other hand, as for the change of jet surface with variation of L_n/D_n, the surface disturbance, the degree of sinuosity, etc. were found to become large gradually with increasing L_n/D_n if the L_n/D_n ratio is smaller than 15 (this value corresponds to the transition L_n/D_n value on the change of Z/D_n as shown in Fig. 1). But, their changes became practically indistinguishable above this range, as seen in the change between 2 and 3 in each jet form. Most of the air entrained by the jets as shown in the form of (A) to (D) is considered to be air entrapped in the surface of the jet[4] or air carried away by the sinuous undulations of the jet[7,14] and so on. One of the causes of almost constant Q_g/Q_L in the nozzles of $L_n/D_n\geqq15$ seems to be

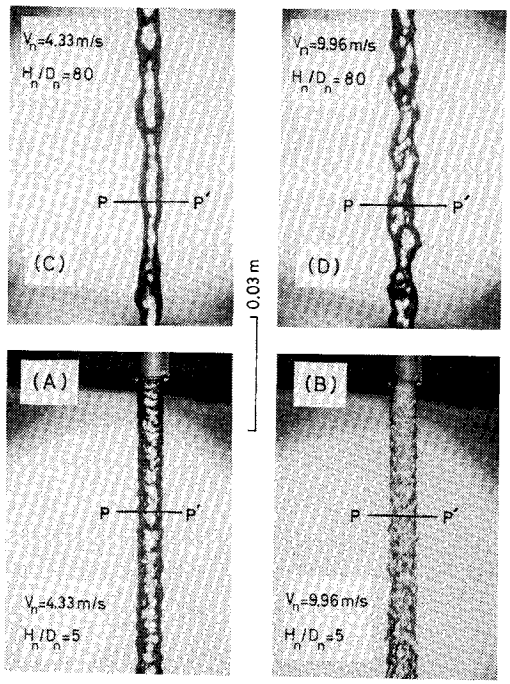

Fig. 10. Photographs of the jet for a nozzle of $D_n=0.007$ m having a value of $L_n/D_n=5$ (the plane P–P' in each jet represnts the position corresponding to the H_n/D_n ratio designated).

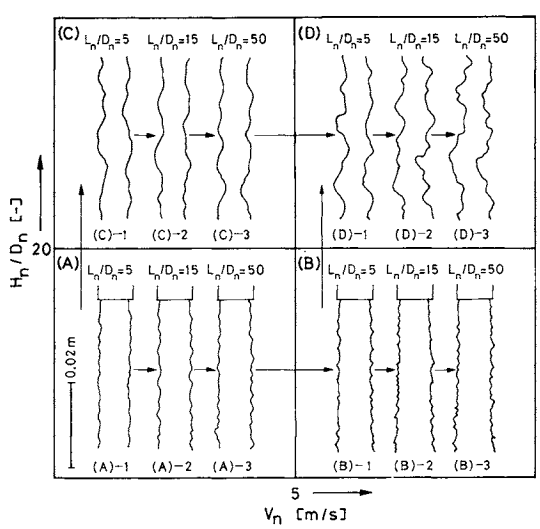

Fig. 11. Schematic representation of jet surface disturbances observed for nozzles of $D_n=0.007$ m having various L_n/D_n ratios under varied conditions of H_n/D_n and V_n [$V_n=4.33$ m/s for (A) and (C) and $V_n=9.96$ m/s for (B) and (D)].

related to the situation that the way of changing of jet surface is almost the same from one to another when such a nozzle was employed at fixed conditions of H_n/D_n and V_n.

Moreover, emphasis is placed here on the fact that the above discussions are based only on surface observations of the jet before plunging. An important factor that must be further taken into consideration is the difference in flow states at the plunging point on the bath surface, as has been reported in a study using inclined water jets.[10] Further studies are necessary, in order to investigate such flow states around the plunging point and to clarify the relationship between their changes and those of the surface of the vertical jet.

Conclusions

The relationship between the bubble penetration depth Z or the gas entrainment rate Q_g and operating conditions such as V_n, H_n and D_n in a vertical plunging jet system where the nozzle length-to-diameter ratio L_n/D_n was varied over a wide range was investigated in an air–water system. When nozzles of $L_n/D_n \geqq 15$ were employed the values of Z and Q_g changed according to V_n, H_n and D_n, but these values were almost independent of L_n/D_n. Based on the results obtained, empirical correlations useful for predicting Z and Q_g under any operating conditions including L_n/D_n were also presented.

Acknowledgment

The authors wish to thank Prof. K. Endoh and Associate Prof. H. Imai of Hokkaido Univ. for their helpful suggestions. Thanks are also due to Prof. M. Fujii of Niigata Univ. for his kind advice.

Nomenclature

D_n	=	nozzle diameter	[m]
F_r	=	Froude number	[—]
g	=	acceleration of gravity	[m/s^2]
H_n	=	nozzle height	[m]
L_n	=	nozzle length	[m]
O_h	=	Ohnesorge number ($=\mu/\sqrt{\rho\sigma D_n}$)	[—]
Q_g	=	volumetric flow rate of entrained gas	[m^3/s]
Q_L	=	volumetric flow rate of liquid fed through the nozzle	[m^3/s]
V_n	=	jet velocity at nozzle exit	[m/s]
Z	=	bubble penetration depth	[m]
ρ	=	density	[kg/m^3]
μ	=	viscosity	[Pa·s]
σ	=	surface tension	[N/m]

Literature Cited

1) Abraham, G.: *J. Hyd. Res.*, **3**, 1 (1965).
2) Bin, A. K. and J. M. Smith: *Chem. Eng. Commun.*, **15**, 367 (1982).
3) Bin, A. K.: Symp. on Scale Effects in Modelling Hyd. Structures, p. 5.5-1, Sept., Germany (1984).
4) Burgess, J. M., N. A. Molloy and M. J. McCarthy: *Chem. Eng. Sci.*, **27**, 445 (1972).
5) Burgess, J. M. and N. A. Molloy: *Chem. Eng. Sci.*, **28**, 183 (1973).
6) Ciborowski, J. and A. K. Bin: *Inzynieria Chemiczna II*, **4**, 557 (1972).
7) Ervine, D. A., E. J. McKeogh and E. M. Elsawy: *Proc. Instn. Civ. Engrs.*, Part 2, **69**, 425 (1980).
8) Kumagai, M. and H. Imai: *Kagaku Kogaku Ronbunshu*, **8**, 1 (1982).
9) Kumagai, M. and K. Endoh: *J. Chem. Eng. Japan*, **15**, 427 (1982).

10) Kumagai, M. and H. Imai: *Kagaku Kogaku Ronbunshu*, **8**, 510 (1982).
11) Kumagai, M. and K. Endoh: *J. Chem. Eng. Japan*, **16**, 74 (1983).
12) McCarthy, M. J., J. B. Henderson and N. A. Molloy: Proc. Chemica. Conf., Australia, Sec. 2, p. 86 (1970).
13) McCarthy, M. J. and N. A. Molloy: *Chem. Eng. Sci.*, **7**, 1 (1974).
14) McKeogh, E. J. and D. A. Ervine: *Chem. Eng. Sci.*, **36**, 1161 (1981).
15) Ohkawa, A., D. Kusabiraki, Y. Kawai, N. Sakai and K. Endoh: *Chem. Eng. Sci.*, **41**, 2347 (1986).
16) Suciu, G. D. and O. Smigelschi: *Chem. Eng. Sci.*, **31**, 1216 (1976).
17) Van de Sande, E. and J. M. Smith: *Chem. Eng. Tech.*, **44**, 1177 (1972).
18) Van de Sande, E. and J. M. Smith: *Chem. Eng. Sci.*, **28**, 1161 (1973).
19) Van de Sande, E.: Ph. D. Thesis, Technische Hogeschool, Delft (1974).
20) Van de Sande, E. and J. M. Smith: *Chem. Eng. J.*, **10**, 225 (1975).
21) Van de Sande, E. and J. M. Smith: *Chem. Eng. Sci.*, **31**, 219 (1976).
22) Yagasaki, T. and T. Kuzuoka: *Res. Rept. of Kōgakuin Univ.*, **47**, 77 (1979).

MATHEMATICAL MODELING OF TRANSDERMAL DRUG DELIVERY

KAKUJI TOJO

Controlled Drug Delivery Research Center, Department of Pharmaceutics, College of Pharmacy, Rutgers University, Piscataway, NJ 08855-0789 U.S.A.

Key Words: Medical Chemical Engineering, Transdermal Drug Delivery, Percutaneous Absorption, Pharmacokinetics, Mathematical Model, Prodrug, Enzymatic Reaction

A dynamic mathematical model for transdermal drug delivery is developed on the basis of the bi-layer skin/two-compartment body model. The effects of metabolism reaction in the viable skin, the drug binding and reservoir function in the stratum corneum, and the solubility and diffusivity of the drug in the skin on the permeation rate-time profile are extensively simulated. The effects of the pharmacokinetic parameters on the plasma concentration profile are also analyzed. The present model is useful not only for analyzing the rate of skin permeation but also for predicting the plasma concentration after transdermal drug delivery.

Introduction

For many years, drugs have been administered percutaneously to achieve localized pharmacological action. Recently, however, the skin has increasingly been used as a portal of entry for systemically active agents. In 1981, ALZA Corporation first introduced a product of transdermal therapeutic systems, Transderm-Scop®, for medication of motion sickness. In 1982, three transdermal delivery systems for nitroglycerin, Nitro-Dur®, Transderm-Nitro® and Nitrodisc, in the treatment of angina pectoris were introduced from Key Pharmaceuticals, Ciba Geigy and G.D. Searle, respectively. In 1985, the transdermal delivery system for clonidine, Catapress-TTS®, was introduced in antihypertensive treatment by Boehringer Ingelheim. Other transdermal drug delivery systems are also in various stages of development and testing. We can expect a significant force of transdermal drug delivery in the near future.

In spite of the great impact of transdermal drug delivery on pharmaceutical society, the mechanism of drug permeation across the skin is not clear due to the complicated structure of the skin. During the last decade, a number of researchers have extensively studied percutaneous absorption of drugs both experimentally and theoretically. They have made great efforts to understand the penetration of drugs through the skin. The permeation data, however, were frequently analyzed on simplistic assumptions such as a single layer skin, a constant diffusivity, a steady-state condition, a simplified boundary condition, a compartment model of skin, etc.[1-3,6,8,9,12-14,18,21,23,37,43,44] A more rigorous approach is needed, at this stage of transdermal drug delivery studies, to elucidate the mechanism of percutaneous absorption.

The main resistance to drug transport across the

Received November 4, 1986. Correspondence concerning this article should be addressed to K. Tojo.